

The behavior of Cu/Cu-C-La₂O₃ nanocomposites prepared by spark plasma sintering: physical and electrochemical properties

M. Amirjan¹, M. Bozorg^{2*}, M. M. Shadkar³

¹*Metallurgy Division, Department of Chemical and Materials Engineering, Niroo Research Institute, Tehran 1468617151, Iran*

²*Department of Chemical & Materials Engineering, Shahrood University of Technology, Shahrood 3619995161, Iran*

³*Politecnico di Torino, Corso Duca degli Abruzzi, Torino 24-10129, Italy*

Received 14 October 2019, received in revised form 9 June 2020, accepted 17 June 2020

Abstract

In the present paper, the effect of La₂O₃ nanoparticle was studied on the physical and electrochemical properties of Cu/Cu-C contacts. The nanocomposite materials were prepared using different La₂O₃ contents (1.0–2.0 wt.%) processed by the spark plasma sintering method. The microstructural observations, density, hardness, electrical resistance measurements, and electrochemical behavior characterization were conducted. The results showed that the hardness, electrical resistance, and corrosion resistance of composites increase with the addition of La₂O₃ nanoparticle.

Key words: rare metal oxide, spark plasma sintering, Cu/Cu-C, contact materials, electrochemical behavior

1. Introduction

Nowadays, copper alloys produced by Spark Plasma Sintering (SPS) are widely used in tribological engineering, like contact wires, bearing, and bushing [1–3]. SPS has some peculiar advantages of quick heating rates, short holding time, and high relative density in a short time. It can also realize the sintering behavior of nano-sized particles without substantial grain growth [4]. Graphite is soft and has low strength. So many researches try to improve the properties of Cu-graphite composites [2, 5, 6]. It has been reported that the sinterability of the composite can be improved by an activated sintering process by adding into small amounts of active elements. Due to its particular outer cell electron structure, the application of rare earth is exposed to many research fields such as optics, tribology [7, 8], etc. Rare earth oxides are considered to be the ideal sintering additive because of their high melting points, chemical stability, excellent mechanical, thermal, optical, and electrical properties [9, 10]. La₂O₃ has a unique electronic structure because that was successfully added into the metal to improve the toughness, strength, and tribological properties [11]. Zhang

et al. showed that by adding extra La₂O₃, the composite possessed better wear resistance [12]. Zhao et al. reported that in the presence of La₂O₃, the corrosion resistance was decreased, and the corrosion current density was increased in the laser clad ferrite-based alloy coatings [13].

In this paper, we make the Cu-C-La₂O₃ composite by SPS method. Our composites include different amounts of La₂O₃-Cu-C. In this research, we have done lots of tests, like SEM, corrosion, and microhardness tests to compare the difference of various composites.

2. Experimental

The copper powder particle ($D_{50} = 63 \mu\text{m}$) with the purity of 99.95%, flake-like graphite particle ($D_{50} = 94 \mu\text{m}$), and La₂O₃ nanoparticles ($< 100 \text{nm}$) were used as precursor materials to prepare the nanocomposites. Figure 1 shows the morphology of used materials. The desired composition, according to Table 1, was first prepared by soft ball milling of blended materials for 2.5 h, and then consolidated us-

*Corresponding author: e-mail address: m.bozorg@shahroodut.ac.ir

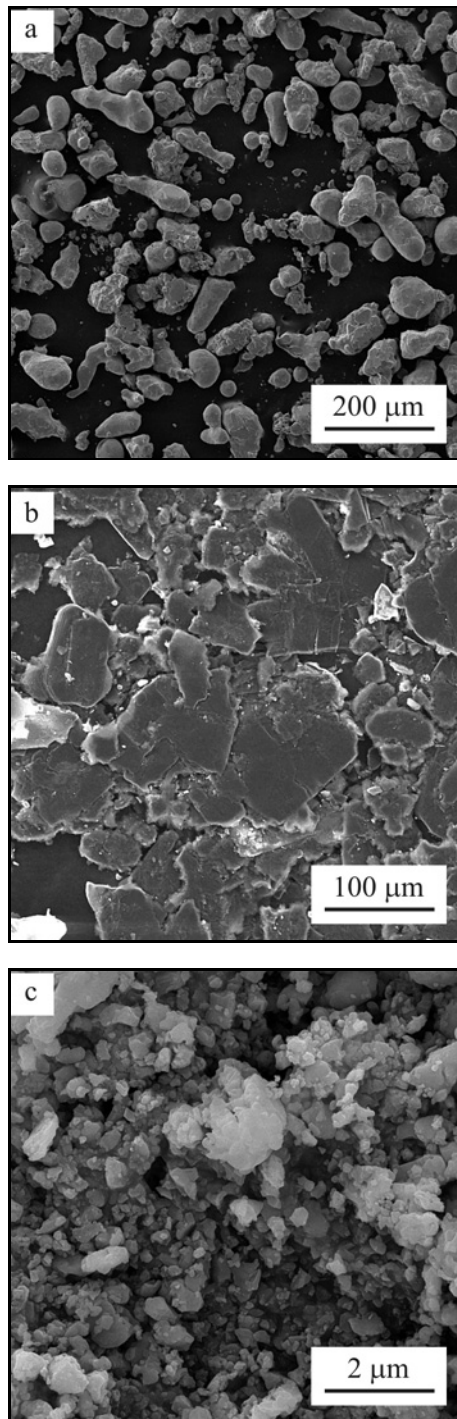


Fig. 1. Primary used materials: (a) Cu powder, (b) graphite powder, and (c) La_2O_3 nanoparticles.

ing the KP spark plasma sintering system. The samples were prepared under 30 MPa pressure at 950 °C for 15 min. The Lantania nanoparticles and graphite contents considered as variables. Then, the samples were cut and prepared for microstructural observation using optical and scanning electron microscopy from the cross-section. The distribution of several phases

Table 1. The investigated samples' specifications

Sample	Composition (wt.%)		
	Cu	C	La_2O_3
Cu	100	–	–
CuC	60	40	–
CuCL1	60	39.0	1.0
CuCL2	60	38.0	2.0

in microstructure was examined by Energy Dispersive Spectroscopy (EDS). Also, the density of compacts was measured using the Archimedes method, according to ASTM B962. The hardness (Brinell, (30gf load for 10 s)) and electrical resistance measurements were conducted on the specimens.

The electrochemical methods were carried out utilizing Ivium vertex. The corrosion behavior of the specimens was investigated in a 3.5 % NaCl solution using EIS and electrochemical polarization. Corrosion tests were performed in a three-electrode cell closed to air under stagnant conditions. A calomel electrode was used as a reference electrode, along with platinum as a counter electrode. The samples were immersed in the test solution for 1500 s to reach the balanced state E_{ocp} . The EIS measurements were immediately performed under measured E_{ocp} , start-up frequency range from 100 kHz to 10 mHz, and amplitude of 10 mV (peak to peak). Potentiodynamic polarization curves were obtained with a scan rate of 1 mV s^{-1} in the potential range of -250 mV relative to the E_{ocp} up to 1 V.

3. Results and discussion

3.1. Microstructure, hardness, and electrical resistance

Figure 2 illustrates the optical micrographs of investigated samples. The grain boundary structure, porosity level, and morphology and distribution of graphite in the Cu matrix can be seen. Also, Figs. 3 and 4 show the scanning electron micrographs and elemental maps for CuC and CuCL1 specimens.

As can be seen, the distribution of composite components in microstructure is homogeneous. Also, the properties of investigated samples are given in Table 2. The relative density values of all samples are higher than 98 %. The hardness decreases from pure copper to copper-graphite samples. This can be due to the presence of a phase with lower hardness.

Nevertheless, the addition of La_2O_3 to composite composition leads to a rise in hardness values, which demonstrates the distributed strengthening effect of

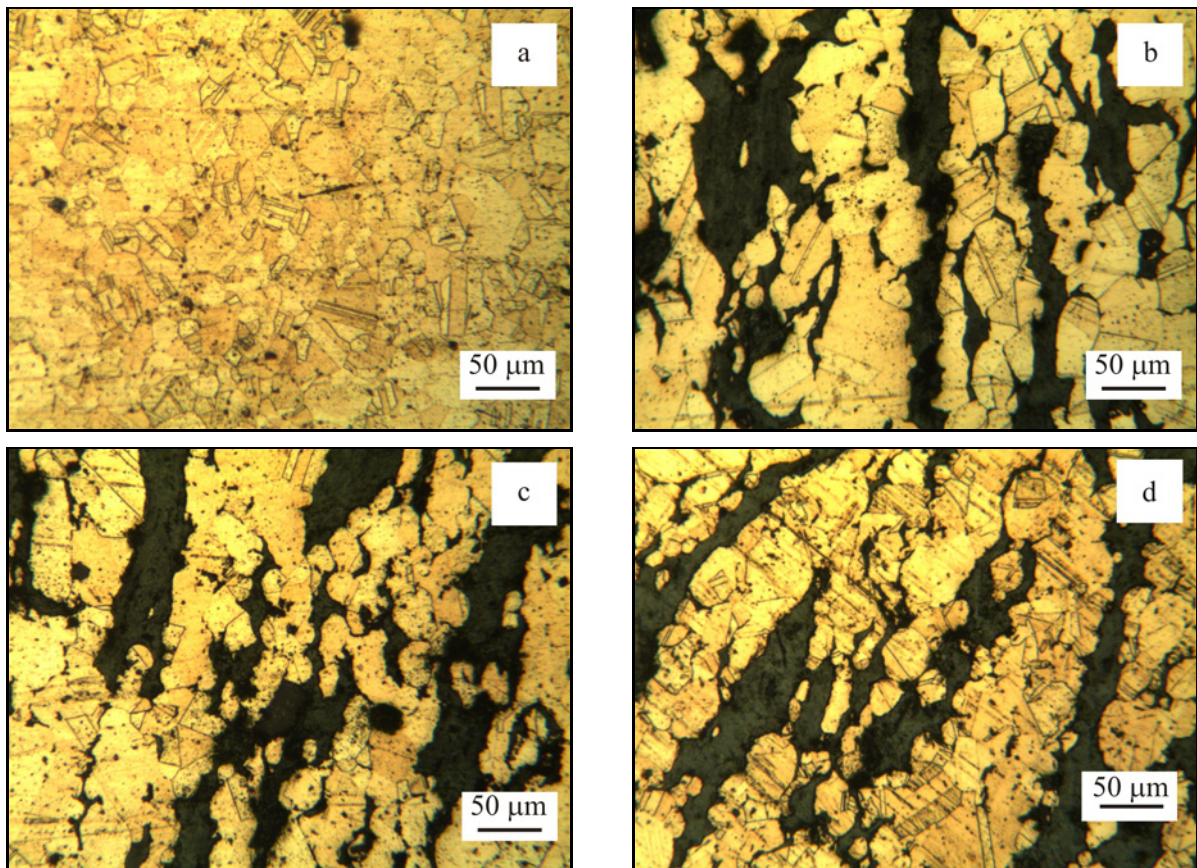


Fig. 2. Optical micrographs of specimens: (a) pure Cu, (b) Cu-C, (c) Cu-C-1.0 La₂O₃, and (d) Cu-C-2.0 La₂O₃.

Table 2. The density, hardness and electrical resistance of investigated samples

Sample	Density		Average grain size (μm)	Hardness HV	Electrical resistivity (Ωm)
	Theoretical (g cm^{-3})	Relative (%)			
Cu	8.96	99.01	50 ± 2	44.67	0.0127
CuC	4.06	98.21	66 ± 3	23.45	0.0306
CuCL1	4.11	98.32	56 ± 2	30.89	0.0479
CuCL2	4.16	98.64	44 ± 2	44.75	0.0673

nanoparticles in the composite. Also, the investigation of microstructure and grain structure shows that the grain size decreases with the addition of reinforcement nanoparticles due to their hindering effects of grain growth. As can be seen in Table 2, an increase in n-La₂O₃ content from 1.0 to 2.0 wt.% leads to a decrease in grain size by about 30 % (from 54 to 38 μm).

The investigation of electrical resistance of the samples revealed a rise in their values for composite samples. The addition of graphite and n-La₂O₃ to the composite composition leads to an increase in electrical resistance because of (1) higher electrical resistivity of graphite/La₂O₃ (100 Ωm) than of pure copper [6], (2) the formation of discontinuity, and decrease of conduction path in samples.

3.2. Electrochemical measurement

Figure 5 shows the Nyquist diagrams of the samples in the NaCl solution. According to Fig. 5, the impedance response of copper-base samples is characterized by one depressing semi-circle at the high frequency (HF) and follows a straight line at low frequency (LF) [14]. It can be seen that the diameter of the Nyquist diagram of those C and La₂O₃ containing alloys is higher than pure copper, suggesting better corrosion behavior [15].

The EIS data were simulated with the electrical equivalent circuit model from previous studies (Fig. 7). In this equivalent circuit, R_s is the solution resistant, R_{ct} is the charge transfer-resistant, CPE rep-

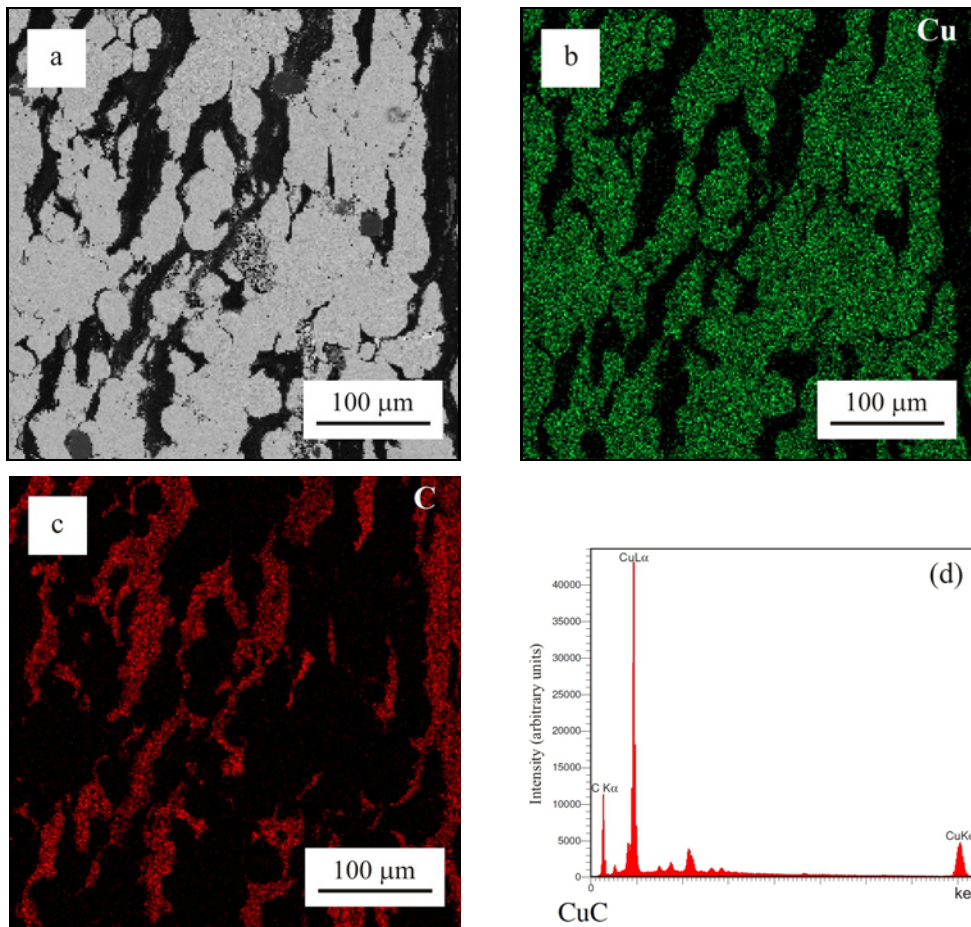


Fig. 3. Scanning electron microscopy and its related elemental map analysis for CuC specimen.

Table 3. Electrochemical impedance parameters for Cu-based samples in NaCl

Sample	R_s ($\Omega \text{ cm}^2$)	CPE ($\text{mS s}^n \text{ cm}^{-2}$)	n	R_{ct} ($\Omega \text{ cm}^2$)	W ($\text{mS}^5 \text{ cm}^{-2}$)
Cu	6.4	5.1	0.86	214.9	2.2
CuC	10.9	3.3	0.85	336.3	11.6
CuCL1	8.8	2.6	0.73	571.5	12.5
CuCL2	11.3	2.2	0.76	640.9	14.2

Table 4. Polarization data of Cu/C- x L samples in 3.5 % NaCl solution

Sample	I_{corr} ($\mu\text{A cm}^{-2}$)	E_{corr} (mV)	β_a (mV dec^{-1})	β_c (mV dec^{-1})
Cu	14.5	-175	42	129
CuC	8.01	-202	40	113
CuCL1	5.32	-257	34	93
CuCL2	3.96	-271	32	91

resents constant phase element, and W is the Warburg diffusion impedance. The electrochemical parameters are calculated by ZSimpWin software and presented in Table 3. According to Table 3, it is found that the

Cu/C- x La₂O₃ alloy has lower capacitance and higher corrosion resistance than pure copper.

For a more detailed evaluation of the behavior of Cu/C composite, the polarization measurement was

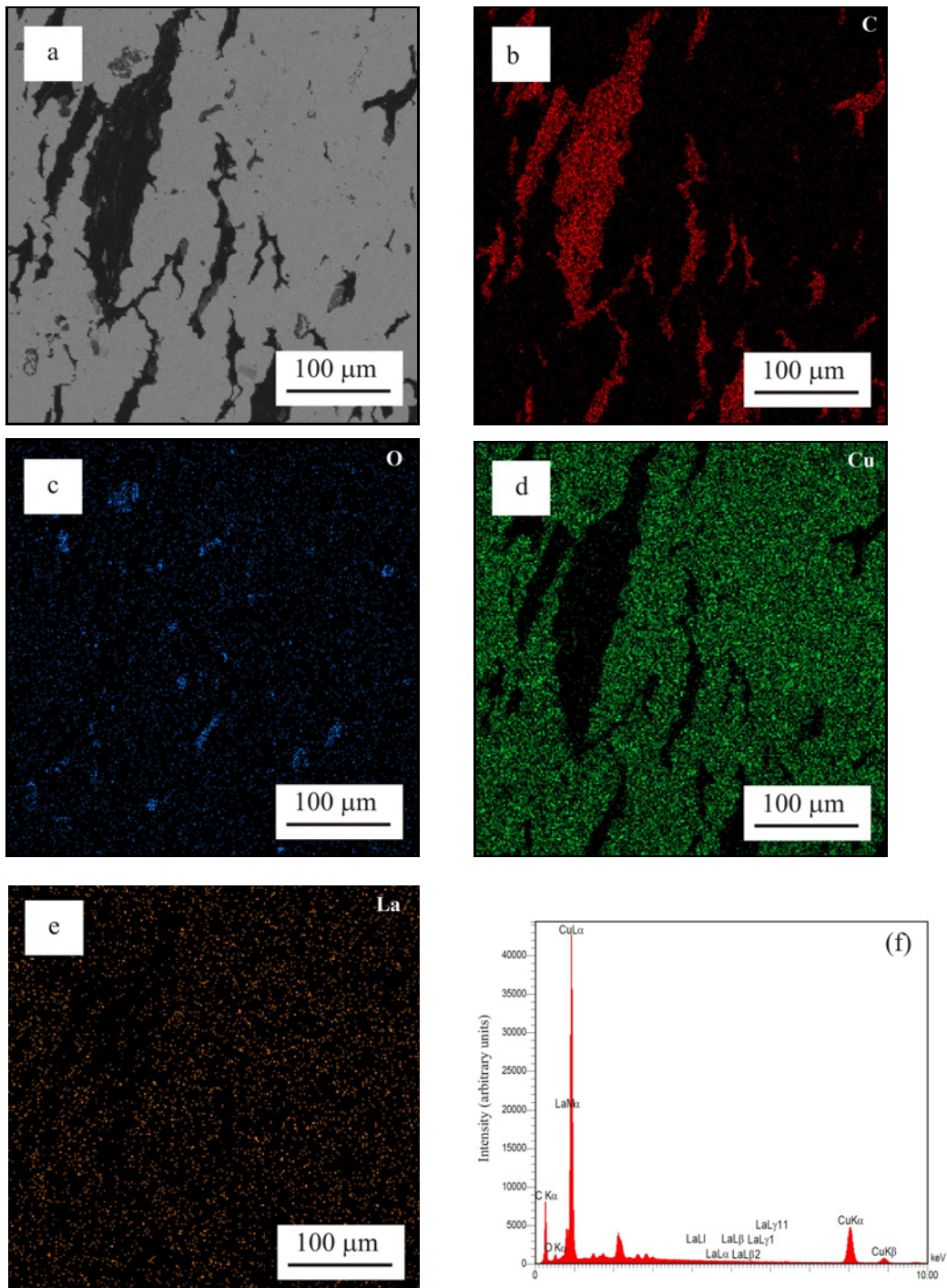


Fig. 4. Scanning electron microscopy and its related elemental map analysis for CuCL1 specimen.

carried out after EIS. The polarization diagrams and polarization data of pure copper and CuC composites are illustrated in Fig. 6 and Table 4, respectively. The polarization diagrams of all samples in the NaCl solution show the typical copper-based materials behavior [16]. Corrosion current density represented lower value for CuCL₂ ($3.96 \mu\text{A cm}^{-2}$) than other samples attesting excellent corrosion resistance. The corrosion

current density for pure copper and Cu/C is 14.5 and $8.01 \mu\text{A cm}^{-2}$, respectively. It has been previously reported that the corrosion resistance of laser clad ferrite-based alloy coatings could be increased significantly by the addition of La₂O₃ [13]. Similar results were reported by a previous study that assessed the effect of the oxide phase on the corrosion behavior of metallic composite [4, 17–19].

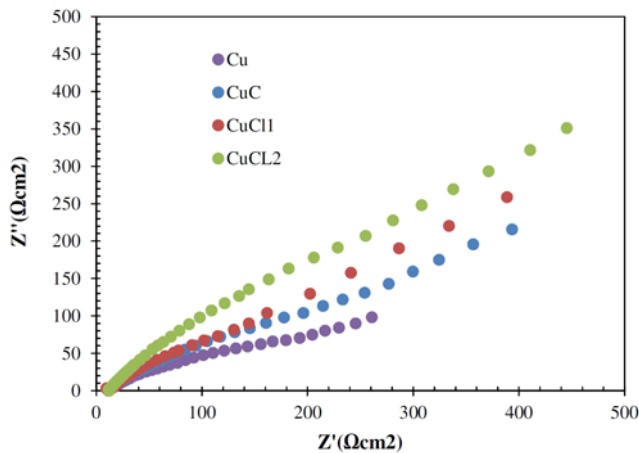


Fig. 5. Nyquist plots of Cu/C- x La₂O₃ samples in 3.5 % NaCl solution.

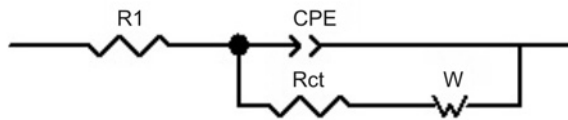


Fig. 6. Potentiodynamic polarization curves for different samples in NaCl solution.

4. Conclusions

The effect of the addition of a different amount of La₂O₃ nanoparticles on the physical and electrochemical properties of Cu/C composites was investigated, and the following results were drawn:

- The microstructure revealed the homogeneous distribution of components in the composite. Also, the grain size decreases with the addition of nanoparticles.
- The electrical resistance and the hardness increase as the n-La₂O₃ are added to the composite composition.
- The electrochemical measurements show that the corrosion resistance of CuCl₂ exhibits the highest corrosion resistance among the tested composites, and the corrosion current density of CuC composites decreases with increasing of La₂O₃.

References

- [1] S. G. Jia, P. Liu, F. Z. Ren, B. H. Tian, M. S. Zheng, G. S. Zhou, Sliding wear behavior of copper alloy contact wire against copper-based strip for high-speed electrified railways, *Wear* 262 (2007) 772–777. [doi:10.1016/j.wear.2006.08.020](https://doi.org/10.1016/j.wear.2006.08.020)
- [2] S. F. Moustafa, S. A. El-Badry, A. M. Sanad, B. Kieback, Friction and wear of copper-graphite composites made with Cu-coated and uncoated graphite powders, *Wear* 253 (2002) 699–710. [doi:10.1016/S0043-1648\(02\)00038-8](https://doi.org/10.1016/S0043-1648(02)00038-8)
- [3] I. Yasar, A. Canakci, F. Arslan, The effect of brush spring pressure on the wear behaviour of copper-graphite brushes with electrical current, *Tribol. Int.* 40 (2007) 1381–1386. [doi:10.1016/j.triboint.2007.03.005](https://doi.org/10.1016/j.triboint.2007.03.005)
- [4] B. Zhang, B. Ma, X. Zhang, Q. Zhu, X. Ren, Y. Zhang, X. Qu, J. Yu, J. Yu, Effects of YSZ and nano-ZrO₂ contents on the properties of Ti2448-ZrO₂ biomedical composites fabricated by SPS, *Ceram. Int.* 44 (2018) 13293–13302. [doi:10.1016/j.ceramint.2018.04.160](https://doi.org/10.1016/j.ceramint.2018.04.160)
- [5] X. Zhang, Y. Zhang, S. Du, Z. Yang, T. He, Z. Li, Study on the tribological performance of copper-based powder metallurgical friction materials with Cu-coated or uncoated graphite particles as lubricants, *Materials (Basel)* 11 (2018) 1–18. [doi:10.3390/ma11102016](https://doi.org/10.3390/ma11102016)
- [6] F. Mo, Y. Feng, Y. Chen, Y. Wang, G. Qian, Y. Dou, X. Zhang, Effect of La₂O₃ on electrical friction and wear properties of Cu-graphite composites, *J. Rare Earths* 33 (2015) 327–333. [doi:10.1016/S1002-0721\(14\)60421-X](https://doi.org/10.1016/S1002-0721(14)60421-X)
- [7] R. Zheng, Z. Zhan, W. Wang, Tribological properties of Cu-La₂O₃ composite under different electrical currents, *J. Rare Earths* 29 (2011) 247–252. [doi:10.1016/S1002-0721\(10\)60440-1](https://doi.org/10.1016/S1002-0721(10)60440-1)
- [8] N. S. Bajaj, S. K. Omanwar, Combustion synthesis and luminescence characteristic of rare earth activated LiCaBO₃, *J. Rare Earths* 30 (2012) 1005–1008. [doi:10.1016/S1002-0721\(12\)60169-0](https://doi.org/10.1016/S1002-0721(12)60169-0)
- [9] F. Agrall, A. K. Jonsher, Dielectric properties of thin films of aluminium oxide and silicon oxide, *Thin Solid Films* 2 (1968) 185–210. [doi:10.1016/0040-6090\(68\)90002-3](https://doi.org/10.1016/0040-6090(68)90002-3)
- [10] R. Ritasalo, M. Antonov, R. Veinthal, S. Hannula, Comparison of the wear and frictional properties of Cu matrix composites prepared by pulsed electric current sintering, *Proc. Est. Acad. Sci.* 63 (2014) 62–74. [doi:10.3176/proc.2014.1.09](https://doi.org/10.3176/proc.2014.1.09)
- [11] M. K. Yoo, Y. Hiraoka, J. Choi, Recrystallization of molybdenum wire doped with lanthanum oxide, *Int. J. Refract. Met. Hard Mater.* 13 (1995) 221–227. [doi:10.1016/0263-4368\(95\)94028-W](https://doi.org/10.1016/0263-4368(95)94028-W)
- [12] H. Zhang, X. Hu, J. Yan, P. Chen, S. Tang, Dry sliding wear behaviors of La₂O₃-WSi₂-MoSi₂ composite against alloy steel, *Wear* 260 (2006) 903–908. [doi:10.1016/j.wear.2005.06.014](https://doi.org/10.1016/j.wear.2005.06.014)
- [13] G. M. Zhao, K. L. Wang, Effect of La₂O₃ on corrosion resistance of laser clad ferrite-based alloy coatings, *Corros. Sci.* 48 (2006) 273–284. [doi:10.1016/j.corsci.2005.01.002](https://doi.org/10.1016/j.corsci.2005.01.002)
- [14] M. Bozorg, T. S. Farahani, J. Neshati, Z. Chaghazardi, G. M. Ziarani, Myrtus communis as green inhibitor of copper corrosion in sulfuric acid, *Ind. Eng. Chem. Res.* 53 (2014) 4295–4303. [doi:10.1021/ie404056w](https://doi.org/10.1021/ie404056w)
- [15] M. Bozorg, A. Ramezani, Characterization and protective performance of acrylic-based nanocomposite coating reinforced with silica nanoparticles, *Mater. Corros.* 68 (2017) 725–730. [doi:10.1002/maco.201609347](https://doi.org/10.1002/maco.201609347)
- [16] M. Amirjan, M. Bozorg, Fabrication and properties of Cu-Al₂O₃ functionally graded nanocomposites prepared by spark plasma sintering: The effect of copper particle size and reinforcement content, *Mater. Res. Express* 6 (2019) 1–10. [doi:10.1088/2053-1591/ab34c5](https://doi.org/10.1088/2053-1591/ab34c5)

- [17] M. Bahraminasab, M. Bozorg, S. Ghaffari, F. Kavakbian, Corrosion of Al_2O_3 -Ti composites under inflammatory condition in simulated physiological solution, Mater. Sci. Eng. C 102 (2019) 200–211. [doi:10.1016/j.msec.2019.04.047](https://doi.org/10.1016/j.msec.2019.04.047)
- [18] M. Mandel, L. Krüger, S. Decker, Electrochemical corrosion studies of spark plasma sintered zirconia particle-reinforced high-alloy steel at different temperatures, Corros. Sci. 90 (2015) 323–330. [doi:10.1016/j.corsci.2014.10.029](https://doi.org/10.1016/j.corsci.2014.10.029)
- [19] M. Bahraminasab, M. Bozorg, S. Ghaffari, F. Kavakbian, Electrochemical corrosion of Ti- Al_2O_3 biocomposites in Ringer's solution, J. Alloys Compd. 777 (2019) 34–43. [doi:10.1016/j.jallcom.2018.09.313](https://doi.org/10.1016/j.jallcom.2018.09.313)